Dinuclear Rhenium Complexes with a Bridging Helicene-bis-bipyridine Ligand: Synthesis, Structure, and Photophysical and Chiroptical Properties

Nidal Saleh, Debsouri Kundu, Nicolas Vanthuyne, Joanna Olesiak-Bańska, Anna Pniakowska, Katarzyna Matczyszyn, V Chang, Gilles Muller, J a Gareth Williams, Monika Srebro-Hooper, et al.

FULL PAPER WILEY-VCH

Dinuclear Rhenium Complexes with a Bridging Helicene-bis-bipyridine Ligand: Synthesis, Structure, and Photophysical and Chiroptical Properties

Nidal Saleh,[a,h] Debsouri Kundu,[a] Nicolas Vanthuyne,[b] Joanna Olesiak-Banska,[c] Anna Pniakowska,[c] Katarzyna Matczyszyn,[c] Victoria Y. Chang,[d] Gilles Muller,[d] J. A. Gareth Williams,[e] Monika Srebro-Hooper,*[,f] Jochen Autschbach,[g] Jeanne Crassous*[,a]

[a] Dr. Nidal Saleh, Debsouri Kundu, Dr. Jeanne Crassous
Univ Rennes, CNRS, ISCR - UMR 6226,
F-35000 Rennes, France.
E-mail: jeanne.crassous@univ-rennes1.fr
[b] Dr. Nicolas Vanthuyne
Aix Marseille University, CNRS Centrale Marseille, iSm2, 13284 Marseille, France.
[c] Dr. Joanna Olesiak-Banska, Anna Pniakowska, Prof. Katarzyna Matczyszyn
Advanced Materials Engineering and Modelling Group, Wroclaw University of Science and Technology, Wrocław, Poland.
[d] Victoria Y. Chang, Dr. Gilles Muller
Department of Chemistry, San José State University, San José, CA 95192-0101, USA.
[e] Prof. J. A. Gareth Williams
Department of Chemistry, Durham University, Durham, DH1 3LE, U.K.
[f] Dr. Monika Srebro-Hooper
Faculty of Chemistry, Jagiellonian University, Gronostajowa 2, 30-387 Krakow, Poland.
E-mail: srebro@chemia.uj.edu.pl
[g] Prof. Jochen Autschbach
Department of Chemistry, University at Buffalo,
State University of New York, Buffalo, New York 14260, USA.
[h] Present address:
Department of Organic Chemistry,
University of Geneva, Geneva, Switzerland.

Supporting information for this article is given via a link at the end of the document.((Please delete this text if not appropriate))

Abstract: By attaching pyridine groups to a diaza[6]helicene, a helical, bis-ditopic, bis-*N^N*-coordinating ligand can be accessed. Dinuclear rhenium complexes featuring this bridging ligand, of the form [{Re(CO)$_3$Cl}$_2$(*N^N–N^N*)], have been prepared and resolved to give enantiopure complexes. They are phosphorescent in solution at room temperature under one- and two-photon excitation. Their experimental chiroptical properties (optical rotation, electronic circular dichroism and circularly polarized emission) have been measured. They show, for instance, emission dissymmetry factors of c.a. ±3.10^{-3}. Quantum-chemical calculations indicate the importance of stereochemistry on the optical activity, pointing towards further design improvements in such types of complexes.

Introduction

N^N-Bidentate ligands incorporating 2,2'-bipyridine (bipy) units are widely used in coordination chemistry and provide a great variety of transition-metal complexes.[1] The latter have been intensively studied for the development of new metal-based luminescent materials and sensing probes.[2] In this context, bipy-based rhenium(I) coordination complexes have been of great interest over the last few decades for their appealing photophysical and photochemical properties. Improved understanding of their excited-state properties and photochemical reactions[3] may indeed potentially lead to biomedical and optoelectronic applications.[4] Since the first report of luminescent rhenium(I) complexes with chelating *N^N*-diimine ligands by Wrighton and Morse,[5] a plethora of studies have demonstrated their desirable features. Among those are efficient emission properties, sizable spin-orbit coupling to promote formally forbidden phosphorescence, absorption in the visible part of the spectrum, large Stokes shifts, resistance to photobleaching, and easy access to hydrosoluble cationic complexes.[6] Exploiting these advantages, Re(I)-tricarbonyl systems have been used in photoredox chemistry,[7] chemi- or electrochemi-luminescence,[8] chemical and biological sensing,[9] bioconjugation,[10] and as phosphorescent dopants for organic light-emitting diodes (OLEDs).[11] In 2015, our groups reported the first examples of rhenium-based phosphors bearing an extended helical π-conjugated 2,2'-bipyridine ligand exhibiting circularly polarized luminescence (CPL) (see systems **Re-3** and **Re-4** in Scheme 1).[12a] Continuing this work, we decided to construct a helical scaffold bearing two bipy units at each extremity, allowing the formation of dinuclear complexes. In this article, we present the synthesis of dinuclear Re(I) complexes

Re-1 and **Re-2**, which differ in the mutual position of chlorine atoms, of general formula [{Re(CO)$_3$Cl}$_2$(**3**)] where **3**, used in either a racemic or an enantiopure form, is 3,14-bis-(2-pyridyl)-4,13-diaza[6]helicene (Scheme 1).[13] The photophysical properties of the enantio-enriched compounds, including luminescence upon one- or two-photon excitation (2PE), together with their chiroptical properties such as optical rotation (OR), electronic circular dichroism (ECD) and CPL, have been measured and interpreted using quantum-chemical calculations.

Results and Discussion

Synthesis of racemic helicenic ligand and its corresponding rhenium(I) complexes

Chiral ligands bearing *N^N*-coordinating units are appealing building blocks for either discrete metallic structures or polymetallic assemblies. However, examples of molecular materials based on chiral bipy ligands and their complexes are still limited.[14] The racemic ligand 3,14-di-(2-pyridyl)-4,13-diaza[6]helicene (±)-**3** was synthesized in two steps as shown in Scheme 1. A double Wittig reaction of naphthalene-2,7-bis(methylenetriphenylphosphonium bromide) [15] **1** with two equivalents of 2,2'-bipyridine-6-carbaldehyde[16] was carried out to obtain the stilbene **2** in 92% yield, as a mixture of *cis* and *trans* isomers, which was then subjected to a double photocyclization reaction to give (±)-diaza[6]helicene **3** (83% yield).[17]

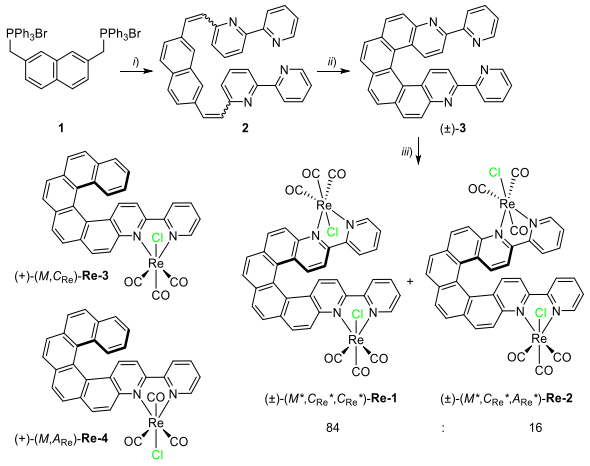

Scheme 1. Synthesis of diaza[6]helicene-bis-bipyridine ligand **3** and dinuclear rhenium(I) complexes (±)-**Re-1** and (±)-**Re-2** in which the metal centres are bridged by **3**; *i*) *n*-BuLi, -78°C, THF then 2,2'-bipyridine-6-carbaldehyde, r.t., overnight, 92%; *ii*) I$_2$ (cat), hν, 700 W Hg lamp, toluene/THF, 4 hrs, 83%; *iii*) Re(CO)$_5$Cl, toluene, reflux, 5 hrs, quant. The structures of corresponding diastereomeric mononuclear Re(I) complexes **Re-3** and **Re-4** are also shown.[12a]

The 3,14-di-(2-pyridyl)-4,13-diaza[6]helicene **3** was fully characterized (see the Supporting Information). It displays the classical spectroscopic features of helicenes. For instance, the complex set of signals in the ^{1}H NMR of the stilbene **2**, associated with different *cis*/*trans* isomers, simplifies upon formation of **3** to give one set of resonances between 7.0 and 8.7 ppm, evidencing its C_2 symmetry (Figure S1.5). Its structure was also confirmed by X-ray diffraction analysis of single crystals grown by slow diffusion of pentane vapors into a dichloromethane solution of the ligand (Figure 1). Compound **3** crystallized in a centro-symmetric space group (C2/*c*) and displays a helical topology (the helicity, or dihedral angle between the two terminal rings, is 61.87°). The two appended 2-pyridyl groups are almost coplanar with the helicenic core (dihedral angles of -11.98° and -10.73°) and the nitrogen atoms within each 2,2'-bipy unit are mutually *trans* to one another. Overall, the helicene-bis-bipyridine **3** exhibits similar features to its parent helicene-mono-bipyridine.[12a]

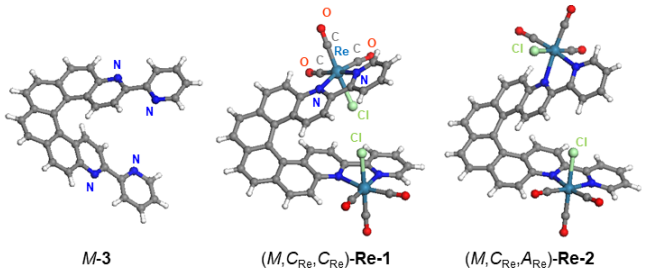

Figure 1. X-ray crystallographic molecular structures of **3**, **Re-1** and **Re-2** (racemic structures, only one enantiomer shown). Deposition Numbers 870779 (for **3**), 875291 (for **Re-1**), 875062 (for **Re-2**), contain the supplementary crystallographic data for this paper. These data are provided free of charge by the joint Cambridge Crystallographic Data Centre and Fachinformationszentrum Karlsruhe Access Structures service www.ccdc.cam.ac.uk/structures.

Re(I) complexes of the form *fac*-[Re(CO)$_3$(*N^N*)Cl], where *N^N* is a diimine ligand such as bipy, can be readily synthesized by reaction of the appropriate ligand with an equimolar amount of Re(CO)$_5$Cl under reflux in non-polar solvents.[12] Accordingly, racemic bis-ditopic ligand (±)-**3** was refluxed with 2 equivalents of Re(CO)$_5$Cl in toluene (see Scheme 1) yielding, after purification by column chromatography, a mixture of dinuclear Re(I) diastereomers (**Re-1**, 84%) and (**Re-2**, 16%), as evidenced by ^{1}H NMR (Figure S1.5) and X-ray diffraction (Figure 1). Obtained by slow diffusion of pentane vapors into CH_2Cl_2 solution, single crystals of complexes **Re-1** and **Re-2** grew in centrosymmetric space groups (**Re-1**: $P2_1/n$; **Re-2**: $P2_1/c$) in which two enantiomeric structures are present. As in previously reported mononuclear Re(CO)$_3$ complexes,[1-3,9,12] each Re atom adopts a distorted octahedral geometry, with the three carbonyl groups being *fac*-oriented around the Re(I). In **Re-1**, both chlorine atoms are directed towards the inner surface of the helicene moiety, resulting in C_2 symmetry, as both Re centers in either enantiomer have either a "*C*" or an "*A*" configuration (see the Supporting Information for a definition), and in a helical angle of 39.13°. In **Re-2**, one of the chlorine atoms is directed inwards giving a "*C*" configuration while the other one directs away from the helicene core with an "*A*" configuration, breaking the symmetry and resulting in a helical angle of 46.39°. Note that there is no evidence in the reaction mixture of the isomer where both the chlorine atoms are directed towards the outer side of the helicene moiety. Thanks to X-ray diffraction analysis, the absolute configuration of each diastereoisomer was determined, namely (*M*,C_{Re},C_{Re})- / (*P*,A_{Re},A_{Re})-**Re-1** and (*M*,C_{Re},A_{Re})- / (*P*,A_{Re},C_{Re})-**Re-2**. The respective C_2 and C_1 symmetry of **Re-1**

and **Re-2** is also reflected in their ^{1}H NMR spectra (see the Supporting Information).

Absorption properties of the helicenic ligand 3 and its Re(I) complexes

The UV/Vis absorption spectrum of **3** in CH_2Cl_2 (5×10^{-5} M, 298 K) shows intense signals ($\varepsilon > 60 \times 10^3$ M^{-1} cm^{-1}) at 272 nm and 286 nm, and several structured bands of lower intensity between 330 and 430 nm (Figure 2a). The incorporation of two Re metal centers into the helicenic ligand is accompanied by a pronounced red-shift in the lowest-energy absorption bands and an increase in molar absorptivity at wavelengths longer than around 375 nm (Table 1). Based on literature assignments for mononuclear $Re(CO)_3$ complexes, the peaks centered at 299 nm are assigned to intraligand (IL) π-π* transitions. The lower energy absorption bands that extend from the near-UV region into the visible one correspond to predominantly IL charge-transfer (CT) excitations with contributions of metal-to-ligand (ML) CT character (*vide infra*).[12,18] To shed light on the nature of the excitations in **Re-1** and **Re-2**, density functional theory (DFT) and time-dependent DFT (TD-DFT) calculations were performed.[19] The computational protocol that was employed followed an approach established in previous research on transition-metal-based systems with helicene ligands.[12a,20] In a nutshell, DFT geometry optimizations were followed by linear response TD-DFT calculations performed with the Becke-Perde[21] and BHLYP[22] exchange-correlation density functionals, respectively, the SV(P) basis with corresponding relativistic core potential for Re atoms,[23] and a continuum solvent model for CH_2Cl_2.[24] See Supporting Information for a complete description of the computational details. Note that, although for smaller molecules basis sets with diffuse functions are generally required to ensure a correct prediction of response properties such as the optical rotation,[33a] for π-conjugated systems with response dominated by valence states, such as helicenes and their derivatives, no dramatic changes in the

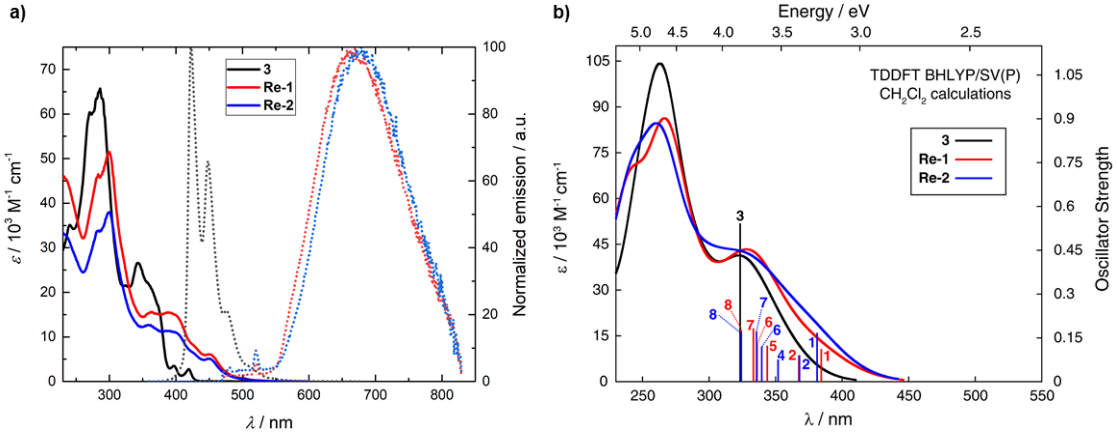

Figure 2. a) Experimental UV/Vis (solid lines) and emission (dotted lines) spectra of **3**, **Re-1**, and **Re-2** in CH_2Cl_2 (~ 10^{-5} M) at r.t. Excitation spectra under these conditions, as well as emission spectra at 77 K, are shown in the Supporting Information. b) Corresponding simulated UV/Vis spectra of **3**, **Re-1**, and **Re-2** with selected calculated excitation energies and oscillator strengths indicated as 'stick' spectra (see also Table 2, Figure 3, and the Supporting Information).

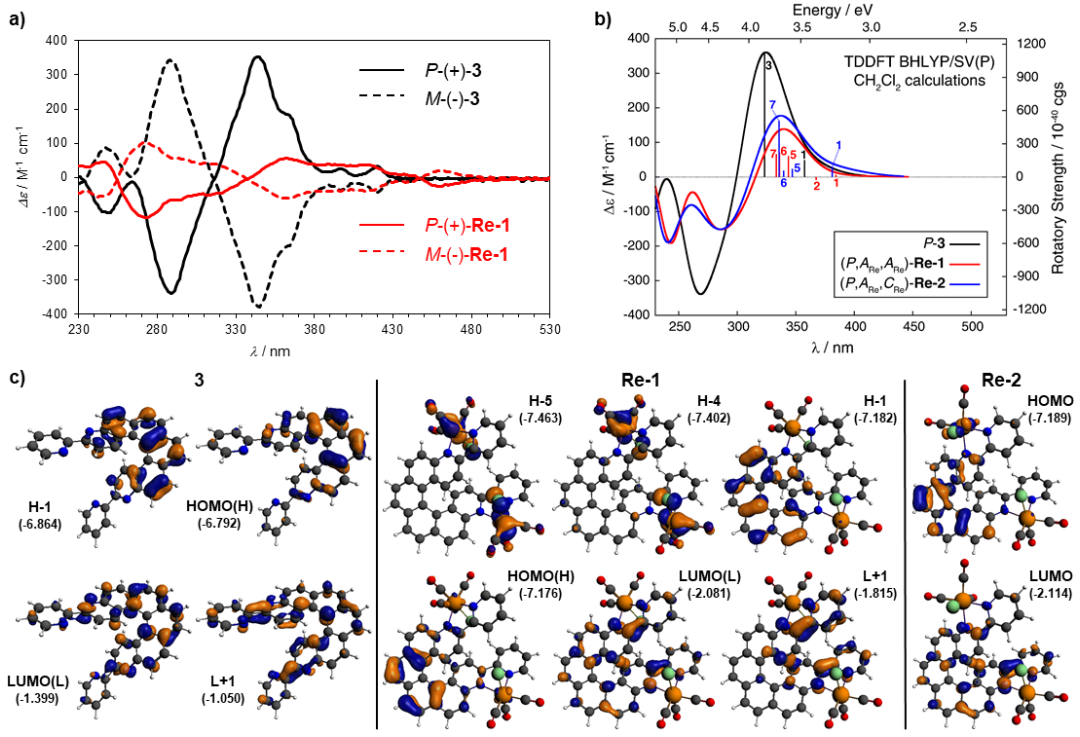

Figure 3. a) Experimental ECD spectra of *P*-(+)- / *M*-(-)-**3** and *P*-(+)- / *M*-(-)-**Re-1** in CH_2Cl_2 (~ 10^{-5} M) at r.t. b) Corresponding simulated ECD spectra of *P*-**3**, (*P*,A_{Re},A_{Re})-**Re-1**, and (*P*,A_{Re},C_{Re})-**Re-2** with selected calculated excitation energies and rotatory strengths indicated as 'stick' spectra (compare with Table 2 and see also the Supporting Information). c) Isosurfaces (0.04 au) of selected molecular orbitals for **3** (left), **Re-1** (middle), and **Re-2** (right); see the Supporting Information for a full set of MOs involved in the intense low-energy excitations of **Re-1** and **Re-2**.

Table 1. Absorption (at 295 K) and emission data (under one-photon excitation at 295 K and at 77 K) of the ligand **3** and the two dinuclear Re complexes.

System	Absorption at 295 K[a]	Emission at 295 K[b]			Emission at 77 K[c]	
	λ_{max} [nm] (ε [M^{-1} cm^{-1}])	λ_{max} [nm]	τ [ns]	$\Phi_{lum} \times 10^2$	λ_{max} [nm]	τ [ns]
(±)-**3**	242 (35100), 272 (60300), 286 (65300), 344 (26500), 366sh (20200), 398 (3500), 420 (2750)	422, 448, 476, 513sh	5.1	8.6[d]	421, 446, 476, 509 [fluor]	8.3
					532, 575, 626, 683[f] [phos]	1.5 x 10^9
(±)-**Re-1**	283 (46500), 299 (51400), 361 (15500), 387 (15400), 450 (6080)	664	38 [36]	0.20[e]	557, 570sh, 604, 624sh, 657	43000
(±)-**Re-2**	283 (33700), 299 (37900), 359 (12700), 389 (11300), 450 (5090)	678	32 [31]	0.15[e]	556, 572, 607, 623sh, 657	47000

[a] In CH_2Cl_2 solution. [b] In deoxygenated CH_2Cl_2 solution; lifetimes in parenthesis are the corresponding values in air-equilibrated solution. [c] In diethyl ether / isopentane / ethanol (2:2:1 v/v). [d] Fluorescence quantum yield measured using quinine sulfate in 1 N $H_2SO_{4\,(aq)}$ as the standard. [e] Phosphorescence quantum yield measured using $[Ru(bpy)_3]Cl_{2\,(aq)}$ as the standard. [f] Bands for the principal vibrational progression only are listed: some additional fine structure is observed (spectra are shown in the Supporting Information).

Table 2. Selected dominant excitations and occupied (occ) – unoccupied (unocc) MO pair contributions (greater than 10%) for (*P*,A_{Re},A_{Re})-**Re-1** and (*P*,A_{Re},C_{Re})-**Re2**.[a]

Excitation	*E* [eV]	λ [nm]	*f*	*R* [10^{-40} cgs]	occ no.	unocc no.	%
				3			
#1	3.47	358	0.079	153.93	H-1 (125)	L (127)	74.1
#3	3.83	323	0.543	1123.13	H (126)	L+1 (128)	70.7
					H-1 (125)	L (127)	11.6
				Re-1			
#1	3.23	384	0.112	23.03	H-1 (199)	L (201)	82.7
#2	3.37	367	0.089	-28.30	H (200)	L (201)	72.7
#5	3.61	344	0.124	191.57	H-4 (196)	L (201)	35.9
					H-1 (199)	L+1 (202)	20.8
					H-5 (195)	L+1 (202)	16.6
					H-3 (197)	L (201)	13.7
#6	3.69	336	0.129	222.42	H-5 (195)	L (201)	52.2
					H-3 (197)	L+1 (202)	18.8
					H-4 (196)	L+1 (202)	17.2
#7	3.72	333	0.183	207.80	H (200)	L+2 (203)	31.0
					H (200)	L+1 (202)	28.3
					H-4 (196)	L+1 (202)	12.3
#8	3.82	324	0.177	-155.56	H-1 (199)	L+1 (202)	45.7
					H-5 (195)	L+1 (202)	18.5
					H-9 (191)	L (201)	10.2

[a] Based on BHLYP/SV(P) continuum solvent (CH_2Cl_2) model calculations. H = HOMO, L = LUMO.

calculated results are expected with an increase in the basis set size.[33b] The resulting simulated UV/Vis spectra of **3**, **Re-1** and **Re-2** are depicted in Figure 2b and show good agreement with the experiments. Namely, the dinuclear Re(I) complexes demonstrate a noticeable decrease in absorption intensity at wavelengths below 300 nm, relative to **3**, and an appearance of additional bands of moderate intensity at longer wavelengths. (The structure, in particular above 350 nm, in the experimental spectra seems to be vibronic in nature, because the broadened vertical excitation spectra in the calculations display far less substructure. Similar considerations apply to the ECD spectra discussed in the following.) Labelled excitations in the low-energy part of the spectra for **3** and **Re-1,2** have been characterized in detail (see ECD analysis below, Table 2, Figure 3, and the Supporting Information for additional calculated results).

Emission of the ligand 3 and the Re(I) complexes under one-photon excitation

At room temperature (rt), compound **3** emits blue fluorescence in solution with 8.6% quantum yield. The 0,0 component is the strongest peak in the vibrationally resolved spectrum, $\lambda_{max}^{fluo}(0,0)$ = 422 nm, and the vibronic progression of approximately 1400 cm^{-1} corresponds to the C=C stretching mode of the helix coupled with C=CH bending (Figure 2 and Table 1). The fluorescence decays monoexponentially with a lifetime τ^{fluo} of 5.1 ns. In a rigid EPA glass at 77 K (Figure S1.1), the fluorescence maxima are essentially unshifted but, in addition, strong, vibronically structured, very long-lived phosphorescence is observed at lower energy, $\lambda_{max}^{phos}(0,0)$ = 532 nm; τ^{phos} = 1.5 s.

The Re(I) complexes **Re-1** and **Re-2** display red phosphorescence in CH_2Cl_2 solution at room temperature (Figure 2 and Table 1). The emission band in each case is broad and structureless, quite typical of classic ^{3}MLCT emitters like $[Ru(bpy)_3]^{2+}$; the emission maximum for **Re-2** is slightly red-shifted by 14 nm compared to **Re-1**. The emission is quite weak (Φ = 0.20 and 0.15% respectively for **Re-1** and **Re-2**) and short-lived (τ^{phos} = 38 and 32 ns respectively), indicative of fast non-radiative deactivation of the triplet excited state that competes effectively with the phosphorescence process. Such features are typical of most $Re(CO)_3(N\text{^}N)Cl$ complexes (for comparison, Re(I) systems **Re-3** and **Re-4** also appeared as weak red-phosphorescent emitters in CH_2Cl_2 at room temperature, *i.e.* **Re-3**: λ_{max}^{phos} = 673 nm, Φ = 0.16%, τ^{phos} = 33 ns, and **Re-4**: λ_{max}^{phos} = 680 nm, Φ = 0.13%, τ^{phos} = 27 ns), the phosphorescence being much weaker than in derivatives where the halide is replaced by a stronger field ligand such as a pyridine or isonitrile.[12a] Owing to the short lifetimes, the phosphorescence is only weakly quenched by O_2 (Table 1). The complexes show very different emission properties at 77 K: the spectra demonstrate very well-defined vibrational structure with $\lambda_{max}^{phos}(0,0)$ substantially blue-shifted, by over 100 nm, compared to λ_{max}^{phos} at 295 K (see Table 1 and Figures S1.2 and S1.3). Moreover, the phosphorescence is very long-lived under these conditions, τ^{phos} > 40 μs. These striking differences between the 77 K and ambient temperature emission properties suggest that the nature of the emissive state is different under the two conditions. The most likely explanation is that, at 77 K, a predominantly ligand-centred $^3\pi$-π^* state lies lower in energy than the ^{3}MLCT state, (CT states being typically destabilised more under low-temperature conditions). Indeed, it is striking how similar are the 77 K phosphorescence spectra of the complexes to the phosphorescence bands of the ligand **3** at 77 K: there is a modest 800 cm^{-1} red-shift of the former (readily attributed to stabilisation of the ligand π^* orbitals arising from binding of the metal cations), but otherwise the profiles are very similar. The influence of the metal ions in promoting the formally forbidden $T_1 \rightarrow S_0$ process is, of course, clear from the shorter lifetimes of the complexes.

Calculated (using TDDFT-BHLYP/SV(P) with a continuum solvent model for CH_2Cl_2) luminescence energies for the ligand **3** and the Re(I) complexes **Re-1** and **Re-2** agree well with the experimental emission data measured at low temperature (see Table S2.4 In particular, the computations correctly reproduce spectral positions of the fluorescence (**3**) and phosphorescence (**3**, **Re-1,2**) maxima with the similar values of $T_1 \rightarrow S_0$ transition energiesobtained for **Re-1** and **Re-2** and their moderate red-shift compared to the phosphorescence of **3**. The MO-pair analysis of the computed phosphorescence transitions also shows that the T_1 excited state for the Re(I) complexes indeed corresponds to the predominantly helicene-centered $^3\pi$-π^* state, very similar to that for **3** although with some clear involvement of the metal orbitals, and confirms that the observed red-shift in its energy relative to the free ligand comes from the stabilization of the helicene π^*-system upon metal complexation (Figures S2.9-10). Finally, we note in passing that the T_1 excited-state optimizations for **Re-1** and **Re-2** performed employing density functionals with a lower fraction of exact exchange led to much lower phosphorescence energies, matching quite well those that were observed experimentally at room temperature, and to the $d_{Re} \mid p_{Cl} \rightarrow \pi^*_{bpy}$ MLCT / XLCT electronic character of the emitting state (see the Supporting Information).

Two-photon emission of the Re-1 complex

Organic dyes with particularly high efficiency of generation of emissive states following two-photon excitation (TPE) (simultaneous absorption of two photons) have been developed in recent years.[25] TPE is an attractive technique for bioimaging in particular, as it provides localized excitation at the focal point of the incident light only, and it allows the use of long wavelengths to which biological tissue is relatively transparent. Metal complexes may possess additional advantages over organic fluorophores in such imaging applications.[26] However, two-photon excited phosphorescence of Re complexes at wavelengths readily available from dye and Ti:Sapphire lasers has rarely been reported in the literature.[27]

The luminescence of **Re-1** under TPE has been measured using a number of excitation wavelengths from 830 to 1000 nm (Figure 4a). Employing the relative fluorescence technique,[28] we calculated the two-photon brightness, $\sigma_{2,eff}$, defined as $\sigma_{2,eff} = \Phi\sigma_2$, where Φ is the photoluminescence quantum yield and σ_2 is the two-photon absorption cross-section (Figure 4b). The values obtained are an order of magnitude lower than $\sigma_{2,eff}$ of standard fluorophores.[29] However, as the photoluminescence quantum yield is only 0.2%, it is clear that **Re-1** is a strong two-photon absorber (*e.g.*, σ_2 = 762 GM at 830 nm). The cross sections are significantly higher than those of purely organic [6]helicenes,[30] illustrating a beneficial effect of metalation on NLO properties.[31]

We attempted to measure the emission of (+)- and (-)-**Re-1** under TPE with right- and left-handed circularly polarized light, generated by a quarter-wave plate placed between the light

source (Ti:Sa laser with femtosecond pulses) and the sample, and thus evaluate two-photon circular dichroism (TPCD) through emission detection. However, the relative differences between TPE luminescence excited with right-handed and left-handed polarized light of the enantiomers were too low to reliably determine TPCD with this technique, which suggests that a method of higher sensitivity, with polarization modulation and lock-in detection of signals, will be required to resolve TPCD of such complexes.

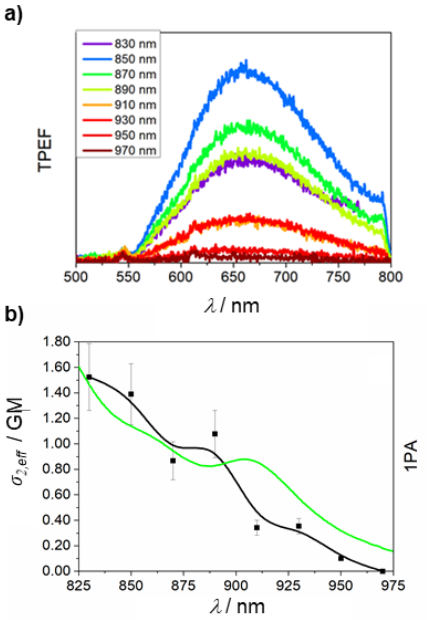

Figure 4. a) Emission spectra of **Re-1** under two-photon excitation at the wavelengths indicated. b) Two-photon brightness $\sigma_{2,eff}$ (black points), compared with the one-photon absorption spectrum (green line) plotted at twice the wavelength.

Electronic circular dichroism (ECD) and optical rotation (OR) of the ligand 3 and the Re(I) complexes

Enantiopure *M*- and *P*-**3** with enantiomeric excesses (*ee* values) between 93 and 99% were obtained by HPLC separation over a chiral stationary phase (Chiralpak IC), with hexane/2-PrOH and 0.1% triethylamine/chloroform (7/1/2) as the mobile phase (see the Supporting Information for details). The enantiopure dinuclear Re(I) complexes were then prepared from enantiopure *M*- and *P*-**3**, respectively. Interestingly, only one enantiopure diastereoisomer (respectively (*M*,C_{Re},C_{Re})-**Re-1** and (*P*,A_{Re},A_{Re})-**Re-1**) was observed in the reaction mixture, *i.e.* enantiopure **Re-2** was not obtained. The different reactivity between enantiopure and racemic mixtures may be explained by the higher solubility of the enantiopure **Re-2** complex formed, which in refluxing toluene may either decompose or transform to thermodynamically more stable **Re-1**. Indeed, according to the DFT calculations, the **Re-1** diastereomer was found to be lower in energy than **Re-2** (by 6.4 kcal mol^{-1} in vacuum and 1.4 kcal mol^{-1} in dichloromethane at the BP/SV(P) level, see the Supporting Information for details). Note that similar differences in reactivity between enantiopure and racemic ligands have already been observed by us in platinum-azahelicene complexes.[32]

[6]Helicene-bis-bipy ligands *M*- and *P*-**3** have high specific and molar optical rotations (ORs) {*P*-(+)-**3**: $[\alpha]_D^{23}$= 4300 degree [dm (g cm^{-3})]$^{-1}$, $[\phi]_D^{23}$= 20830 degree cm^2 dmol^{-1} (± 5%) at *C* 4 x 10^{-5} M in CH_2Cl_2}. These values are more than double those of [6]helicene-bipy[12a] that can be explained by the more extended π-conjugated system in **3**, as also evidenced in the ECD spectrum (*vide infra*). Surprisingly, complex (*P*,A_{Re},A_{Re})-(+)-**Re-1** displays a much lower molar rotation value {$[\phi]_D^{23}$ = 4500 degree cm^2 dmol^{-1} (± 5%) at *C* 5 x 10^{-5} M in CH_2Cl_2} than the pristine ligand *P*-(+)-**3**. This might be due to a mismatch effect between the stereochemistry of the chiral metal center and of the helicene. It should be however noted that a direct comparison of OR for **Re-1** (and **Re-2**, see below) vs. **3** may not be fully sensible, as the data for the complexes may be affected by anomalous dispersion. The computed (using BHLYP/SV(P) with a continuum solvent model for CH_2Cl_2) molar rotations, with *ca.* 19500 and 4100 degree cm^2 dmol^{-1} obtained for *P*-**3** and (*P*,A_{Re},A_{Re})-**Re-1**, respectively (see Table S2.1), agree very well with experiment. Importantly, the calculations also indicate that higher OR values might be expected for **Re-2** than **Re-1** (*ca.* 11500 degree cm^2 dmol^{-1} was computed for (*P*,A_{Re},C_{Re})-**Re-2**), confirming a presence of a strong match/mismatch stereochemistry effect in the considered systems. The analysis of the calculated **Re-1** and **Re-2** structures shows that the aforementioned effect may be a consequence of a modification of π-stacking-like interactions between the terminal rings of the helicenic ligand in each diastereomer resulting from the different arrangements of the ancillary CO and Cl ligands around the metal center observed for both Re stereochemistries. In **Re-1**, which has both chloride atoms directed towards the inner surface of the helicene moiety and stabilized by the attractive interactions with hydrogen atoms of the *N^N* fragments, the bipyridine units are visibly closer to each other than in **Re-2**, in which one of the chlorides points away from the helicene (and one CO is directed inwards), an arrangement that places the bipyridine units farther away from each other and weakens their π-stacking-like interactions (see Figure S2.1). This is also clearly reflected in the helicities observed in the solid state (*vide supra*, 39.13 and 46.39° for **Re-1** and **Re-2**, respectively). As an increase in the helical pitch of the helicenic moiety tends to increase the magnitude of the optical rotation,[33] **Re-2** should (and computationally does) exhibit higher OR values than **Re-1**.

The comparison of experimental ECD between the ligand and complexes is displayed in Figure 3a. *P*-(+)-**3** shows a strong negative band at 289 nm ($\Delta\varepsilon$ = -278 M^{-1} cm^{-1}) and strong positive one at 341 nm ($\Delta\varepsilon$ = +290 M^{-1} cm^{-1}) accompanied by weaker bands between 380 and 430 nm. (+)-**Re-1** and (-)-**Re-1** display mirror-image spectra, in which several bands of medium intensities appear ((+)-**Re-1**: $\Delta\varepsilon$ ~ -70, -30, +45, +30, -12 M^{-1} cm^{-1} at 272, 313, 361, 411 and 459 nm, respectively). The corresponding computed broadened ECD spectra (BHLYP/SV(P) with a continuum solvent model for CH_2Cl_2) for the *P*-isomers of **3**, **Re-1** and **Re-2** are displayed in Figure 3b. Considering that no vibronic contribution has been taken into account, which is known to be often present in helicenic systems,[34] the calculations account for the main observed bands, demonstrating – again – the notable red-shift, and a

significantly decreased intensity of the **Re-1** spectrum compared to that for **3** (*vide supra*).

The molecular orbital (MO) pairs assignment of low-energy intense excitations for **3** and **Re-1** is provided in Table 2. Figure 3c shows the corresponding MOs that are dominantly involved in the transitions (see also the Supporting Information). The analysis revealed that the main positive intensity observed in the ECD spectra of **Re-1** originates from excitations no. 5, 6, and 7 calculated at between 345 and 330 nm. The excitations are of MLCT and XLCT character (metal, halogen (X = Cl) → helicene-bis-bipyridine charge transfer engaging both metal fragments) type with minor helicenic intraligand CT (excitations no. 5 and 6). In the case of excitation no. 7 the participating MOs indicate a predominance of π-π* and ILCT transitions localized in the helicene-bis-bipyridine moiety with some admixture of (M+X)LCT. Such strong involvement of other than 'helical' helicene π-orbitals in these excitations rationalizes the substantial decrease in ECD intensity of **Re-1** compared to **3**. The lowest-energy part of the simulated spectrum is due to two excitations (no. 1 and 2, calculated at 384 and 367 nm, respectively) that correspond mainly to π-π* transitions within the helicenic ligand and demonstrate rather weak, comparable, rotatory strength values of opposite signs thus cancelling each other in the broadened spectrum. Consequently, the weak negative band at low-energy in the experimental (+)-**Re-1** ECD is not present in the spectrum computed with solvent effects. However, it appears in the corresponding gas-phase calculated spectrum (see Figure S2.2). A more sophisticated solvent model and / or an inclusion of vibronic effects that were shown in some cases to be indeed responsible for a change in the chiral response sing of an electronic excited state,[34b,35] are likely needed to ensure a correct description of this band.

As seen in Figure 3b, the complexes **Re-1** and **Re-2** display generally similar spectral envelopes of the calculated ECD spectra, except that the spectrum for **Re-2** is overall more intense at longer wavelengths. This rationalizes the larger optical rotation value calculated for **Re-2**. The analysis of the MO-pair contributions to the dominant excitations for **Re-2** shows that their assignment is overall similar to those in **Re-1** (see Table S2.3 and Figure S2.8). In **Re-2**, however, for the metal center comprising the chloride pointing away from the helicene, stronger π-conjugation between the helical ligand and the metal fragment is visible in the MOs, due to an evidently more favorable relative spatial orientation of both moieties (see for example the isosurfaces of the HOMO in Figure 3c and HOMO-1 in the the Supporting Information). Accordingly, for **Re-2** (vs. **Re-1**) the Re(I) d orbitals become more involved in the intense dominantly helicene π-π* and ILCT excitations (such as no. 1 and no. 7 calculated at 381 and 336 nm, respectively). This correlates with significantly larger rotatory strength (*R*) values of the excitations compared to **Re-1** that account for the higher intensity of the ECD spectrum. A comparative analysis of the magnitudes of *R* for such excitations in terms of their underlying electric and magnetic transition dipole moments vectors (Table S2.5 and Figure S2.12) indicates that the enhancement can be traced back to an increased deviation of the angle between these vectors from 90°, imposed by a larger helical pitch of the helicene moiety in **Re-2** that is reinforced by the different arrangement of the CO and Cl ligands around one metal center relative to the other (*vide supra*).

CPL activity of the ligand 3 and the Re-1 complex

We resorted to CPL spectroscopy[36] to investigate the polarization of the emitted light of the enantiopure pairs of the starting ligand **3** and of the rhenium(I) complex **Re-1**. Almost mirror-image CPL spectra were obtained in degassed dichloromethane solutions at room temperature, with respective luminescence dissymmetry factor g_{lum} values of +0.0086/-0.0084 at ~450 nm for *P*-(+)-**3**/*M*-(-)-**3** and of +0.0034/-0.0030 for (*P*,A_{Re},A_{Re})-(+)-**Re-1**/(*M*,C_{Re},C_{Re})-(-)-**Re-1** around the emission maximum at ~630 nm (see Figure 5). These results are in line with our previous findings on CPL-active helicene-mono-bipyridine system and its corresponding neutral and cationic phosphorescent rhenium complexes reported in Reference 12a ($|g_{lum}|$ values between 0.0013 and 0.0034). This confirms the capability to design helicenic organic fluorophors and rhenium-based phosphors that exhibit CPL activity.[12a,37] It is interesting to note that for **Re-1** the sign of the CPL signal is opposite to that of the lowest-energy band in ECD (g_{abs} = -0.0065 for (*P*,A_{Re},A_{Re})-(+)-**Re-1**), which suggests that the electronic states involved in the corresponding absorption and emission processes are different and / or the transition is not Franck−Condon allowed.[34b]

Conclusion

Dinuclear Re(I)-based complexes bearing a bis-ditopic helicene-bis-bipy ligand have been prepared in racemic and enantiopure forms. They displayed one- and two-photon phosphorescence. The combination of helical *P*/*M* chirality of the helicenic ligand with the *A*/*C* stereochemistries at the two rhenium centers enabled the close examinaton of their effect on the chiroptical properties, namely OR, ECD and CPL activity. Overall experimental and theoretical studies reveal that bimetallic Re(I) complexes display similar performances to their monometallic analogues. The results indicate that future directions for improved characteristics of Re(I) systems should probably be towards cationic complexes, in which more intense emission is usually observed, with a controlled match/mismatch stereochemistry effect.

Acknowledgements

We thank the Ministère de l'Education Nationale, de la Recherche et de la Technologie, the Centre National de la Recherche Scientifique (CNRS), the ANR (10-BLAN-724-1-NCPCHEM and 12-BS07-0004-METALHEL-01). J.A. acknowledges the Center for Computational Research (CCR) for computational resources, and grant CHE-1855470 from the National Science Foundation for financial support. M.S.-H. thanks the PL-Grid Infrastructure and the ACC Cyfronet AGH in Krakow, Poland for providing computational resources. G.M. thanks the NIH, Minority Biomedical Research Support (1SC3GM089589-08) and the Henry Dreyfus Teacher-Scholar Award for financial support. D.K. thanks the European Commission Research Executive Agency (Grant Agreement number: 859752 — HEL4CHIROLED — H2020-MSCA-ITN-2019) for financial support.

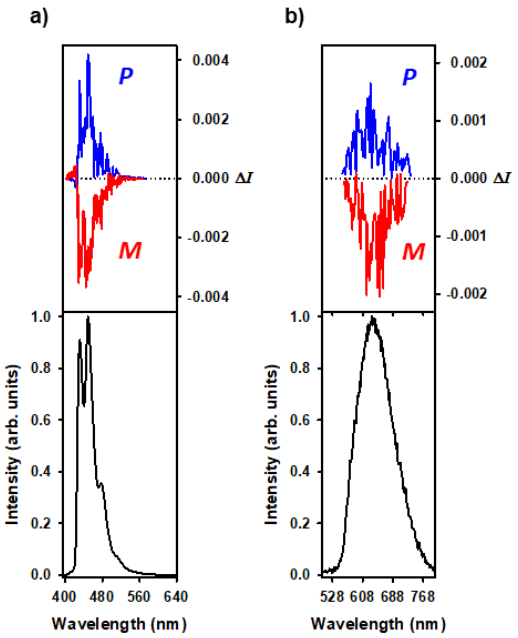

Figure 5. CPL (upper curves) and total luminescence (lower curves) spectra of a) **3** and b) **Re-1** enantiomers (blue for (+) and red for (-)), in degassed dichloromethane solution (2 mM) at 295 K, upon excitation at 381-382 nm and 448-457 nm, respectively.

Keywords: circularly polarized luminescence • helicenes • N ligands • rhenium • two-photon absorption

References

[1] a) G. Chelucci, R. P. Thummel, *Chem. Rev.* **2002**, *102*, 3129-3170; b) H.-L. Kwong, H.-L. Yeung, C.-T. Yeung, W.-S. Lee, C.-S. Lee, W.-L. Wong, *Coord. Chem. Rev.* **2007**, *251*, 2188-2222.

[2] a) H. Le Bozec, V. Guerchais, (eds.) *Molecular Organometallic Materials for Optics*, *Topics in Organometallic Chemistry series*, Springer, **2009**; b) H. Yersin, (ed.) *Highly Efficient OLEDs with Phosphorescent Materials*, Wiley VCH, **2008**.

[3] V. W.-W. Yam, K. M.-C. Wong, *Chem. Comm.* **2011**, *47*, 11579-11592.

[4] C.-C. Ko, A. W.-Y. Cheung, L. T.-L. Lo, J. W.-K. Siu, C.-O. Ng, S.-M. Yiu, *Coord. Chem. Rev.* **2012**, *256*, 1546-1555.

[5] M. Wrighton, D. L. Morse, *J. Am. Chem. Soc.* **1974**, *96*, 998-1003.

[6] a) K.-C. Chang, S.-S. Sun, A. J. Lees, *Inorg. Chim. Acta* **2012**, *389*, 16-28; b) L. C.-C. Lee, K.-K. Leung, K. K.-W. Lo, *Dalton Trans.* **2017**, *46*, 16357-16380; c) K. K.-W. Lo, *Acc. Chem. Res*. **2015**, *48*, 2985-2995; d) K. K.-W. Lo, W.-K. Hui, C.-K. Chung, K. H.-K. Tsang, T. K.-M. Lee, D. C.-M. Ng, *J. Chin. Chem. Soc.* **2006**, *53*, 53-65; e) K. K.-W. Lo, M.-W. Louie, K. Y. Zhang, *Coord. Chem. Rev.* **2010**, *254*, 2603-2622; f) K. K.-W. Lo, K. H.-K. Tsang, K.-S. Sze, C.-K. Chung, T. K.-M. Lee, K. Y. Zhang, W.-K. Hui, C.-K. Li, J. S.-Y. Lau, D. C.-M. Ng, N. Zhu, *Coord. Chem. Rev.* **2007**, *251*, 2292-2310; g) K. K.-W. Lo, K. Y. Zhang, S. P.-Y. Li, *Eur. J. Inorg. Chem.* **2011**, 3551-3568; h) V. W.-W. Yam, Chem. Commun. 2001, 789-796; i) A. M.-H. Yip, K. K.-W. Lo, *Coord. Chem. Rev.* **2018**, *361*, 138-163.

[7] a) H. Tsubaki, A. Sekine, Y. Ohashi, K. Koike, H. Takeda, O. Ishitani, *J. Am. Chem. Soc.* **2005**, *127*, 15544-15555; b) D. Beck, J. Brewer, J. Lee, D. McGraw, B. A. DeGraff, J. N. Demas, *Coord. Chem. Rev.* **2007**, *251*, 546-553.

[8] a) M. M. Richter, Chem. Rev. 2004, 104, 3003-3036; b) S. Y. Reece, M. R. Seyedsayamdost, J. Stubbe, D. G. Nocera, *J. Am. Chem. Soc.* **2006**, *128*, 13654-13655.

[9] 1 a) K. K.-W. Lo, W.-K. Hui, C.-K. Chung, K. H.-K. Tsang, D. C.-M. Ng, N. Zhu, K.-K. Cheung, *Coord. Chem. Rev.* **2005**, *249*, 1434-1450; b) V. Fernández-Moreira, F. L. Thorp-Greenwood, M. P. Coogan, *Chem. Comm*. **2010**, *46*, 186-202.

[10] K. K.-W. Lo, K. H.-K. Tsang, N. Zhu, *Organometallics* **2006**, *25*, 3220-3227; b) K. K.-W. Lo, W.-K. Hui, C.-K. Chung, K. H.-K. Tsang, T. K.-M. Lee, C.-K. Li, J. S.-Y. Lau, D. C.-M. Ng, *Coord. Chem. Rev.* **2006**, *250*, 1724-1736.

[11] N. J. Lundin, A. G. Blackman, K. C. Gordon, D. L. Officer, *Angew. Chem. Int. Ed.* **2006**, *45*, 2582-2584.

[12] a) N. Saleh, M. Srebro, T. Reynaldo, N. Vanthuyne, L. Toupet, V. Y. Chang, G. Muller, J. A. G. Williams, C. Roussel, J. Autschbach, J. Crassous, *Chem. Comm.* **2015**, *51*, 3754-3757; b) N. Saleh, B. Moore, II, M. Srebro, N. Vanthuyne, L. Toupet, J. A. G. Williams, C. Roussel, K. K. Deol, G. Muller, J. Autschbach, J. Crassous, *Chem. Eur. J.* **2015**, *21*, 1673-1681; c) J. Chen, J.; B. Captain, N. Takenaka, *Org. Lett.* **2011**, *13*, 1654-1657; d) J. Klívar, M. Šámal, A. Jančařík, J. Vacek, L. Bednárová, M. Buděšínský, P. Fiedler, I. Starý, I.; I. G. Stará, *Eur. J. Org. Chem.* **2018**, 5164-5178; e) H. Isla, N. Saleh, J.-K. Ou-Yang, K. Dhbaibi, M. Jean, M. Dziurka, L. Favereau, N. Vanthuyne, L. Toupet, B. Jamoussi, M. Srebro-Hooper, J. Crassous *J. Org. Chem.* **2019**, *84*, 5383-5393.

[13] See other examples of helicenic di-rhenium complexes: a) E. Quartapelle Procopio, D. Dova, S. Cauteruccio, A. Forni, E. Licandro, M. Panigati, *ACS Omega* 2018, *3*, 11649-11654; b) J. M. Fox, T. J. Katz, *J. Org. Chem.* **1999**, *64*, 302-305.

[14] a) C. Kaes, A. Katz, M. W. Hosseini, *Chem. Rev.* **2000**, *100*, 3553-3590; b) J. Crassous, *Chem. Soc. Rev.* **2009**, *38*, 830-845; c) J. Crassous, *Chem. Comm.* **2012**, *48*, 9684-9692; d) Y. H. Zhou, J. Li, T. Wu, X. P. Zhao, Q. L. Xu, X. -L. Li, M. -B. Yu, L. L. Wang, P. Sun, Y. X. Zheng, *Inorg. Chem. Commun.* **2013**, *29*, 18-21.

[15] A. Terfort, H. Görls, H. Brunner, *Synthesis* **1997**, 79-86.

[16] a) Y.-Q. Fang, G. S. Hanan, *Synlett* **2003**, *6*, 852-854; b) A. Ramírez-Monroy, T. M. Swager, *Organometallics* **2011**, *30*, 2464-2467.

[17] Note that racemic helicene-bis-bipy ligand 3 was recently used by us to prepare a dinuclear dysprosium complex behaving as a field-induced single molecule magnet in the crystalline phase, see: J. Flores Gonzalez, V. Montigaud, N. Saleh, O. Cador, L. Ouahab, J. Crassous, B. le Guennic, F. Pointillart, *Magnetochemistry* **2018**, *4*, 39.

[18] a) M. I. Azocar, L. Mikelsons, G. Ferraudi, S. Moya, J. Guerrero, P. Aguirre, C. Martinez, *Organometallics* **2004**, *23*, 5967-5974; b) M. R. Feliz, F. Rodriguez-Nieto, G. Ruiz, E. Wolcan, J. *Photochem. Photobiol., A* **1998**, *117*, 185-192; c) G. Pourrieux, F. Fagalde, I. Romero, X. Fontrodona, T. Parella, N. E. Katz, *Inorg. Chem.* **2010**, *49*, 4084-4091; d) T. Rajendran, B. Manimaran, F.-Y. Lee, G.-H. Lee, S.-M. Peng, C. M. Wang, K.-L. Lu, *Inorg. Chem.* **2000**, *39*, 2016-2017; e) K. A. Walters, K. D. Ley, C. S. P. Cavalaheiro, S. E. Miller, D. Gosztola, M. R. Wasielewski, A. P. Bussandri, H. van Willigen, K. S. Schanze, *J. Am. Chem. Soc.* **2001**, *123*, 8329-8342; f) V. W.-W. Yam, B. Li, Y. Yang, B. W.-K. Chu, K. M.-C. Wong, K.-K. Cheung, *Eur. J. Inorg. Chem.* **2003**, 4035-4042; g) T. Yu, D. P.-K. Tsang, V. K.-M. Au, W. H. Lam, M.-Y. Chan, V. W.-W. Yam, *Chem. Eur. J.* **2013**, *19*, 13418-13427.

[19] a) M. Srebro-Hooper, J. Autschbach, *Annu. Rev. Phys. Chem.* **2017**, *68*, 399-420; b) J. Autschbach, *Chirality* **2009**, *21*, E116-E152.

[20] a) S. Graule, M. Rudolph, N. Vanthuyne, J. Autschbach, C. Roussel, J. Crassous, R. Réau, *J. Am. Chem. Soc.* **2009**, *131*, 3183-3185; b) E. Anger, M. Srebro, N. Vanthuyne, C. Roussel, L. Toupet, J. Autschbach, R.

Réau, J. Crassous, *Chem. Commun.* **2014**, *50*, 2854-2856; c) N. Saleh, B. Moore, II, M. Srebro, N. Vanthuyne, L. Toupet, J. A. G. Williams, C. Roussel, K. K. Deol, G. Muller, J. Autschbach, J. Crassous, *Chem. Eur. J.* **2015**, *21*, 1673-1681; d) M. Srebro, E. Anger, B. Moore, II, N. Vanthuyne, C. Roussel, R. Réau, J. Autschbach, J. Crassous, *Chem. Eur. J.* **2015**, *21*, 17100-17115; e) N. Hellou, M. Srebro-Hooper, L. Favereau, F. Zinna, E. Caytan, L. Toupet, V. Dorcet, M. Jean, N. Vanthuyne, J. A. G. Williams, L. Di Bari, J. Autschbach, J. Crassous, *Angew. Chem. Int. Ed.* **2017**, *56*, 8236-8239; f) E. S. Gauthier, L. Abella, N. Hellou, B. Darquié, E. Caytan, T. Roisnel, N. Vanthuyne, L. Favereau, M. Srebro-Hooper, J. A. G. Williams, J. Autschbach, J. Crassous, *Angew. Chem. Int. Ed.* **2020**, *59*, 8394-8400.

[21] a) A. D. Becke, *Phys. Rev. A* **1988**, *38*, 3098-3100; b) J. P. Perdew, *Phys. Rev. B* **1986**, *33*, 8822-8824; c) J. P. Perdew, *Phys. Rev. B* **1986**, *34*, 7406.

[22] a) C. Lee, W. Yang, R. G. Parr, *Phys. Rev. B* **1988**, *37*, 785-789; b) A. D. Becke, *J. Chem. Phys.* **1993**, *98*, 1372-1377.

[23] a) A. Schäfer, H. Horn, R. Ahlrichs, *J. Chem. Phys.* **1992**, *97*, 2571-2577; b) K. Eichkorn, F. Weigend, O. Treutler, R. Ahlrichs, *Theor. Chem. Acc.* **1997**, *97*, 119-124; c) D. Andrae, U. Häußermann, M. Dolg, H. Stoll, H. Preuß, *Theoret. Chim. Acta* **1990**, *77*, 123-141.

[24] J. Tomasi, B. Mennucci, R. Cammi, *Chem. Rev.* **2005**, *105*, 2999-3093.

[25] M. Pawlicki, H. A. Collins, R. G. Denning, H. L. Anderson, *Angew. Chem. Int. Ed.* **2009**, *48*, 3244-3266.

[26] Y. Chen, R. Guan, C. Zhang, J. Huang, L. Ji, H. Chao, *Coord. Chem. Rev.* **2016**, *310*, 16-40 and references therein.

[27] a) J. R. Lakowicz, F. N. Castellano, I. Gryczynski, Z. Gryczynski, J. D. Dattelbaum, *J. Photochem. Photobiol. A: Chem*. **1999**, *122*, 95-101; b) E. Ferri, D. Donghi, M. Panigati, G. Prencipe, L. D'Alfonso, I. Zanoni, C. Baldoli, S. Maiorana, G. D'Alfonso, Emanuela Licandro, *Chem. Commun.* **2010**, *46*, 6255-6257

[28] V. Grande, C. Shen, M. Deiana, M. Dudek, J. Olesiak-Banska, K. Matczyszyn, F. Wurthner, *Chem. Sci.* **2018**, *9*, 8375-8381.

[29] N. S. Makarov, M. Drobizhev, A. Rebane, *Opt. Express* **2008**, *16*, 4029-4047.

[30] C. Dıaz, Y. Vesga, L. Echevarria, I. G. Stara, I. Starỳ, E. Anger, C. Shen, M. El Sayed Moussa, N. Vanthuyne, J. Crassous, A. Rizzo, F. E. Hernandez, *RSC Adv.* **2015**, *5*, 17429-17437.

[31] J. Massue, J. Olesiak-Banska, E. Jeanneau, C. Aronica, K. Matczyszyn, M. Samoc, C. Monnereau, C. Andraud, *Inorg. Chem.* **2013**, *52*, 10705-10707.

[32] a) D. Mendola, N. Saleh, N. Vanthuyne, C. Roussel, L. Toupet, F. Castiglione, T. Caronna, A. Mele, J. Crassous, *Angew. Chem. Int. Ed.* **2014**, *53*, 5786-5790; b) D. Mendola, N. Saleh, N. Hellou, N. Vanthuyne, C. Roussel, L. Toupet, F. Castiglione, F. Melone, T. Caronna, F. Fontana, J. Marti-Rujas, E. Parisini, L. Malpezzi, A. Mele, J. Crassous, *Inorg. Chem.* **2016**, *55*, 2009-2017.

[33] a) M. Srebro, N. Govind, W. A. de Jong, J. Autschbach, *J. Phys. Chem. A* **2011**,*115*, 10930-10949; b) M. El Sayed Moussa, M. Srebro, E. Anger, N. Vanthuyne, C. Roussel, C. Lescop, J. Autschbach, J. Crassous, *Chirality* **2013**, *25*, 455-465.

[34] a) O. E. Weigang Jr., J. A. Turner, P. A. Trouard, *J. Chem. Phys.* **1966**, *45*, 1126-1134; b) Y. Liu, J. Cerezo, G. Mazzeo, N. Lin, X. Zhao, G. Longhi, S. Abbate, F. Santoro, *J. Chem. Theory Comput.* **2016**, *12*, 2799-2819; c) Q. Xu, Y. Liu, X. Zhao, S. Chen, Q. Li, M. Wang, C. Yang, *Spectrochim. Acta A*, **2020**, *231*, 118132; d) Y. Liu, Q. Xu, J. Sun, L. Wang, D. He, M. Wang, C. Yang, *Spectrochim. Acta A*, **2020**, *239*, 118475.

[35] a) N. Lin, Y. Luo, F. Santoro, X. Zhao, A. Rizzo, *Chem. Phys. Lett.* **2008**, *464*, 144-149; b) N. Lin, F. Santoro, X. Zhao, A. Rizzo, V. Barone, *J. Phys. Chem. A* **2008**, *112*, 12401-12411; c) G. Pescitelli, V. Barone, L. Di Bari, A. Rizzo, F. Santoro, *J. Org. Chem.* **2013**, *78*, 7398-7405.

[36] a) F. S. Richardson and J. P. Riehl, *Chem. Rev.* **1977**, *77*, 773-792; b) J. P. Riehl and F. S. Richardson, *Chem. Rev.* **1986**, *86*, 1-16; c) J. P. Riehl, G. Muller in N. Berova, P. L. Polavarapu, K. Nakanishi, R. W. Woody, *Comprehensive chiroptical spectroscopy: applications in stereochemical analysis of synthetic compounds, natural products, and biomolecules*; John Wiley & Sons, 2012, vol. 1, pp 65-90; d) J. Kumar, T. Nakashima, T. Kawai, *J. Phys. Chem. Lett.* **2015**, *6*, 3445-3452; e) B. Kunnen, C. Macdonald, A. Doronin, S. Jacques, M. Eccles and I. Meglinski, *J. Biophotonics* **2015**, *8*, 317-323; f) E. M. Sánchez-Carnerero, A. R. Agarrabeitia, F. Moreno, B. L. Maroto, G. Muller, M. J. Ortiz, S. de la Moya, *Chem. Eur. J.* **2015**, *21*, 13488-13500; g) G. Longhi, E. Castiglioni, J. Koshoubu, G. Mazzeo, S. Abbate, *Chirality* **2016**, *28*, 696-707; h) H. Tanaka, Y. Inoue, T. Mori, *ChemPhotoChem* **2018**, *2*, 386-402; i) J. Han, S. Guo, H. Lu, S. Liu, Q. Zhao and W. Huang, *Adv. Opt. Mater.* **2018**, *6*, 1800538; j) R. Carr, N. H. Evans, D. Parker, *Chem. Soc. Rev.* **2012**, *41*, 7673-7686; k) F. Zinna, L. Di Bari, *Chirality* **2015**, *27*, 1-13 ; l) D. -W. Zhang, M. Li, C. -F. Chen, *Chem. Soc. Rev.* **2020**, *49*, 1331-1343 ; m) B. Doistau, J. -R. Jiménez, C. Piguet, *Front. Chem.* **2020**, *8*, 555.

[37] a) W.-L. Zhao, M. Li, H.-Y. Lu, C.-F. Chen, *Chem. Commun.* **2019**, *55*, 13793-13803; b) *Circularly polarized luminescence in helicene and helicenoid derivatives* (chap. 4) J. Crassous in *Circularly Polarized Luminescence of Isolated Small Organic Molecules*, T. Mori (ed.), Springer, **2020**.

10.1002/cplu.202000559

WILEY-VCH

Entry for the Table of Contents

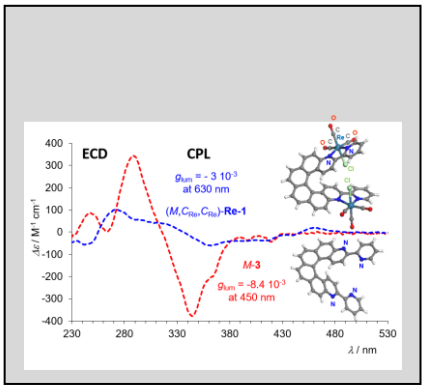

Enantiopure Re(I) complexes have been prepared from enantiopure helical bis-bidentate bis-bipy ligands and their photophysical and chiroptical properties, including two-photon emission, have been studied.

Institute and/or researcher Twitter usernames: ((optional))